Atmos. Chem. Phys. Discuss., 8, 17467–17493, 2008
www.atmos-chem-phys-discuss.net/8/17467/2008/

Atmospheric Chemistry and Physics Discussions

This discussion paper is/has been under review for the journal *Atmospheric Chemistry and Physics (ACP)*. Please refer to the corresponding final paper in *ACP* if available.

Ozone Monitoring Instrument spectral UV irradiance products: comparison with ground based measurements at an urban environment

S. Kazadzis[1,2], A. Bais[2], A. Arola[3], N. Krotkov[4], N. Kouremeti[2], and C. Meleti[2]

[1]Finnish Meteorological Institute, Research and Development, Helsinki, Finland
[2]Laboratory of Atmospheric Physics, Aristotle University Thessaloniki, Thessaloniki, Greece
[3]Finnish Meteorological Institute, Research and Development, Kuopio, Finland
[4]Goddard Earth Sciences and Technology Center, University of Maryland, Baltimore County, Baltimore, MD, USA

Received: 8 July 2008 – Accepted: 27 August 2008 – Published: 24 September 2008

Correspondence to: S. Kazadzis (stylianos.kazantzis@fmi.fi)

Published by Copernicus Publications on behalf of the European Geosciences Union.

Abstract

We have compared spectral ultraviolet overpass irradiances from the Ozone Monitoring Instruments (OMI) against ground-based Brewer measurements at Thessaloniki, Greece from September 2004 to December 2007. It is demonstrated that OMI overestimates UV irradiances by 30%, 17% and 13% for 305 nm, 324 nm, and 380 nm respectively and 20% for erythemally weighted irradiance. The bias between OMI and Brewer increases with increasing aerosol absorption optical thickness. We present methodologies that can be applied for correcting this bias based on experimental results derived from the comparison period and also theoretical approaches using radiative transfer model calculations. All correction approaches minimize the bias and the standard deviation of the ratio OMI versus Brewer ratio. According to the results, the best correction approach suggests that the OMI UV product has to be multiplied by a correction factor $C_A(\lambda)$ are in the order of 0.8, 0.88 and 0.9 for 305 nm, 324 nm and 380 nm respectively. Limitations and possibilities for applying such methodologies in a global scale are also discussed.

1 Introduction

During the past decades a lot of effort has been put into composing global UV irradiance climatology datasets using ground based (GB) measurements from different locations (WMO, 2007). However, due to the limited availability of long term UV data series, combined with the fact that GB measurements cover a small fraction of the Earth's surface, satellite sensors are widely used for estimating UV irradiance reaching the ground from ozone and reflectivity measurements, have gained particular attention. The development of satellite UV estimation techniques have been among the most important scientific issues within the UV community during the previous years (e.g. Krotkov et al., 2002). Following the many successful years that Total Ozone Mapping Spectrometer (TOMS) has been providing global UV irradiance measurements,

ACPD

8, 17467–17493, 2008

the Ozone Monitoring Instrument started providing global UV data since September 2004 (Tanskanen et al., 2007).

OMI is a Dutch-Finnish instrument that flies on NASA's Aura Mission as part of the Earth Observation System (EOS) launched in July 2004. AURA is part of a constellation of satellites known as the A-Train. OMI is a contribution of the Netherlands's Agency for Aerospace Programs (NIVR) in collaboration with the Finnish Meteorological Institute (FMI) to the EOS Aura mission and provides information on various atmospheric parameters (Levelt et al., 2006), such as ozone, aerosols, clouds, surface UV irradiance and other trace gasses. OMI is a wide swath, nadir viewing, near-UV and visible spectrograph that measures solar ultraviolet and visible reflected and backscattered radiation in the range 270–500 nm (Levelt et al., 2006). The spatial resolution of the measurements is $13\times24\,km^2$ in nadir and larger towards the edges of the swath.

One of the goals of OMI is the investigation of changes in global surface UV irradiance. Surface UV estimates based on satellite data have been used extensively in the last decade to establish global UV climatologies and to examine possible long-term changes in surface UV (WMO, 2007 and references therein). The OMI surface UV algorithm consists of a calculation for clear sky cases extended with corrections in the case of cloudy pixels (or ones containing non-absorbing aerosols) (Tanskanen et al., 2006). In the real atmosphere, provided that cloud screening procedures are accurately taken into account, the accuracy of the UV product is limited by the imperfect knowledge of aerosol properties and pollutants mainly in the boundary layer. Cloud effects have also a large impact in the UV retrieval from OMI and in addition they need to be accurately detected for reliable OMI aerosol retrieval. The small pixel-size of OMI, as compared with TOMS, is a major advantage for cloud screening. The validation of satellite-derived UV products against GB measurements is an essential task in order to assess their accuracy. Several validation studies with heritage TOMS satellite instrument (e.g. Herman et al., 1999; Fioletov et al., 2002; Kazantzidis et al., 2006) revealed a positive bias in many locations, with the satellite derived UV being higher. It was also observed that satellite UV agrees much better with the GB measurements

ACPD
8, 17467–17493, 2008

at pristine sites (Lauder, in New Zealand (McKenzie et al., 2001), or Canadian West coast (Fioletov et al., 2002) than in more polluted European and North-American sites (Kazantzidis et al., 2006). Therefore, it was suggested that at least part of the bias could be attributed to the boundary layer aerosol absorption, not accounted for in the current satellite UV algorithm (Krotkov et al., 2002; Arola et al., 2005).

Lately, Tanskanen et al. (2008) focused on the validation of the widely used daily erythemally weighted irradiance. The satellite-derived erythemal daily doses were compared with those derived from the ground-based measurements at 17 sites and 18 instruments. The main objectives of this study were to discuss the applicability of the OMI data for surface UV monitoring and to establish a more accurate cloud correction method for UV retrieval. One of their conclusions, confirmed also by Ialongo et al., 2008, is that the OMI UV aerosol absorption plays an important role in the UV radiation levels reaching the ground and for such cases OMI overestimates the calculated surface UV irradiance levels, especially at urban areas, by 20% to 40%. With regard to the spectral aspect, Wuttke et al. (2003) emphasized the importance of spectral comparisons within validation studies as a mean to provide possible hints about the sources of uncertainties.

In this study we focus on comparing OMI and GB UV spectral measurements at different wavelengths at the urban aerosol environment of Thessaloniki, Greece. The difference at each wavelength is quantified and categorized according to the presence of clouds or aerosols in the area. Furthermore, we investigate possible off-line correction formulas in order to take into account aerosol absorption effects that influence the OMI UV.

2 Materials and methods

2.1 Ground based measurements

At the Laboratory of Atmospheric Physics, Aristotle University of Thessaloniki (AUTH), a monitoring program for spectral solar irradiance measurements has been in operation since 1989, using a Brewer MK III (290–365 nm, 0.5 nm step) spectroradiometer (Garane et al., 2006). In addition, direct irradiance spectra under cloud-free conditions and total ozone measurements have been used to derive aerosol optical thickness (AOT) (Kazadzis et al., 2007). The monitoring program includes a suite of other radiometric measurements and observations that are used for the characterization of the atmospheric conditions during the measurements. These ancillary measurements include: solar irradiance at 302, 312, 320, 340 and 380 nm and erythemal irradiance from two NILU-UV multi-filter radiometers, erythemal irradiance from a YES UVB-1 radiometer, shortwave solar irradiance from a Kipp & Zonnen CM 21 pyranometer and sky images sampled every 5 min. These data sets have been used to compare irradiance measurements at the surface with the overpass irradiance data calculated from OMI measurements.

The monitoring station is located at the center of the city of Thessaloniki which is the second largest city in Greece, with a population of 1.2 million, and is bounded to the north by the Balkan countries and to the south by the Aegean Sea. Thessaloniki is affected by both anthropogenic and natural emission sources (Kazadzis et al., 2007). Local emissions and regional pollution transport contribute to the poor air quality of the city which is reflected mostly in particulate matter (PM) concentrations. The 24 h limit values for PM_{10} (50 μgr/m^3) are exceeded for more than half of the days during a year in the city centre's environmental monitoring sites. The amount of aerosols in this location is quite high, with a annual mean AOT at 340 nm equal to 0.45 and monthly values ranging between 0.3 and 0.7, for winter and summer months, respectively (Kazadzis et al., 2007).

Comparisons of GB data with OMI products were conducted for the spectral irra-

ACPD
8, 17467–17493, 2008

diance at 305, 324, 380 nm and for the CIE weighted dose rate using GB averaged irradiance measurements performed within ±15 min from the OMI overpass time. It is well known that satellite derived surface irradiance is greatly affected by clouds and under such conditions comparisons with GB measurements at a single point is always challenging. For this reason, the comparisons were separated in cloud-free and all-skies data sets. Cloud free cases have been determined using the classification of the ground based measurements using pyranometer data (Vassaras et al., 2001), in combination with meteorological hourly sky observations.

Brewer spectroradiometer UV data were corrected for wavelength shifts using the SHICRIVM algorithm (Slaper et al., 1995). The OMI derived spectral irradiance data are reported at the same spectral resolution with the GB measurements (0.55 nm full width at half maximum). As the Brewer spectra are measured up to 365 nm, the irradiance data at 380 nm was constructed from each measured spectrum using the SHICRIVM algorithm. The time series of the OMI – GB irradiance were analyzed and the possible differences that could depend on various parameters such as: solar zenith angle, ozone, time, presence of clouds and aerosols, were investigated.

The AOT information was taken into consideration in the following analysis only for clear sky days and only when at least one GB measurement was available within ±30 min from OMI overpass time. The associated single scattering albedo (SSA) was retrieved at 340 nm using the methodology described in Bais et al., 2005. Model calculations were performed using the Libradtran (Mayer and Kylling, 2005) package, in order to construct look up tables (LUT) of the ratio of UV irradiances, under aerosol free and actual aerosol conditions.

2.2 OMI UV retrieval methodology

The OMI surface UV algorithm is an extension of the TOMS UV algorithm developed at NASA Goddard Space Flight Center (GSFC) (Eck et al., 1995; Krotkov et al., 1998; Herman et al., 1999; Krotkov et al., 2001; Tanskanen et al., 2006). The OMI surface UV algorithm is used for offline production of the global surface UV data using as input

the OMI TOMS total column ozone (Bhartia and Wellemeyer, 2002) and reflectance at non-absorbing wavelength (360 nm). The common approach involves estimation of the clear-sky surface irradiance E_{clear} which is adjusted to actual surface irradiance by using a satellite derived cloud/aerosol transmittance factor C_T:

$$E_{cloud} = E_{clear} C_T \quad (1)$$

The a-priori surface albedo information required for modeling of the surface UV irradiance is not point-wise surface albedo but rather a regional quantity, referred to as effective albedo, and describes the overall effect of the surface albedo of the surrounding area on the surface UV irradiance. The radiative transfer model involves a climatological set of latitude-dependent ozone and temperature profiles. Krotkov et al. (1998) describe the details of the model and assumptions used in determination of the clear-sky irradiance. They conclude that in the absence of clouds, aerosols, and snow cover, the satellite estimates of the surface UV can have accuracies comparable to the GB measurements. Additional information on clear sky modeling approaches can be found in Tanskanen et al. (2008). For the calculation of C_T, Krotkov et al. (2001) presented two alternative cloud correction methods: (1) based on modified Lambertian Equivalent Reflectivity (LER) model (Eck et al., 1995) and (1) based on homogeneous plane-parallel C1 cloud layer. LER is determined by solving a simple form of the radiative transfer equation that assumes a pure Rayleigh scattering atmosphere bounded by an isotropically scattering Lambertian surface (e.g., Bhartia et al., 1993) at terrain pressure, and C_T is estimated from equation:

$$C_T = \frac{1 - \mathrm{LER}}{1 - R_s} \quad (2)$$

where R_s is surface albedo.

Absorbing aerosols (e.g., organic carbon, smoke, and dust) or trace gases (e.g., NO_2, SO_2) are known to lead to systematic overestimation of the surface UV irradiance (Krotkov et al., 1998; Arola et al., 2005; Chubarova, 2004). The current OMI surface UV algorithm assumes no aerosol absorption. In this work we introduce an additional

aerosol absorption correction factor C_A that can be applied to post-correct operational OMI UV data as follows:

$$E\,\mathrm{corr} = C_A * E_{cloud} = C_A * E_{clear} C_T \quad (3)$$

The C_A is defined to be equal unity in case of non-absorbing aerosols (sulfate, sea salt) and less than unity in case of absorpbing aerosols (i.e. dust, carbonaceous, pollution). In this paper we provide and compare several algorithms for estimating C_A, which can be later applied for a post correction of the operational OMI UV data according to Eq. (3) to account for aerosol absorption effects.

3 Results

3.1 Validation statistics

The comparison of the Brewer spectroradiometer GB measurements and OMI standard UV product (E_{cloud}) was assessed by studying the OMI/GB ratio (RT). The histograms of RT are plotted for each of the three wavelengths and the CIE dose rate separately. The distributions were analyzed by calculating the median value of RT (m). Additionally we have determined the percentage of the satellite-derived data that agrees within ±10 and ±20% with the reference data (denoted as W_{10} and W_{20}, respectively). Cloudless cases statistics are also presented. In addition, and only for cloudless cases, GB measurements are compared with E_{clear} to assess the calculated C_T that for this cases includes only aerosol scattering correction.

The validation statistics are presented in Table 1. Together with the median and the W_{10} and W_{20} the coefficient of determination (R^2) is presented.

Results of Fig. 1 and Table 1 show an overall overestimation of the Ecloud compared with the GB measurements. The bias is larger for shorter wavelengths. The bias slightly increases (10%–15%) for all sky (cloudless or cloudy) conditions compared to the clear sky cases (Table 1). Also, the W_{10} and W_{20} percentages are dropped by

approximately 10%. For the cloud free cases the coefficient of determination is higher than 0.9, while W_{20} percentages reach 90% for all cases. It has to be mentioned that total number of cases (days) analyzed was 810 while 267 of them were cloud free. Concerning the comparison (shown last column of Table 1) with the E_{clear} model calculations from OMI algorithm (1), it has to be noted that differences among E_{clear} and Brewer GB on cloudless conditions are in the order of 2–3% which are the levels of the correction that is included in the OMI UV algorithm for non-absorbing aerosol effects. In order to evaluate additional correction methodologies for absorbing aerosols we have been using the above dataset and measured results for the area of Thessaloniki.

4 Aerosol effects

4.1 UV attenuation due to aerosols

The Thessaloniki area is characterized by strongly aerosol load, with particularly absorbing aerosols and increased air pollution (Bais et al., 2005; Koukouli et al., 2006; Amiridis et al., 2005). Thus it can easily be argued that the degree of overestimation of the Thessaloniki OMI surface UV irradiance under cloudless conditions is mainly due to the aerosol absorbing layers not taken into account in the OMI UV algorithm.

Three year monthly mean AOT and total ozone climatological data from Thessaloniki have been used as inputs to the Libradtran radiative transfer model to calculate the attenuation of UV irradiance at 324 nm due to aerosols (Fig. 2). The SSA used for these calculations was set to 0.90 at 340 nm. Figure 2 also shows the bias between operational OMI UV (Ecloud) and GB measurements, under cloud free conditions.

According to the statistics presented in Table 1, 77% of the measurements are within the ±10% range shown in the right part of Fig. 2. Figure 2 shows just an example of comparing the magnitude of the UV attenuation due to aerosols with the OMI–GB differences. The deviation of the two curves during the winter months is most probably due to the constant SSA used in the model calculations. Arola et al. (2005) have shown

ACPD
8, 17467–17493, 2008

that for the Thessaloniki area and during the period 1997–2003 SSA in the UV is lower, hence signifying higher absorption, during wintertime.

4.2 Investigation of possible post-correction methods

Based in the above results, in this section we investigate various methodologies that could probably be used for correcting this aerosol absorption effect on the OMI retrieved UV products and to calculate C_A. For this purpose the Aerosol Absorption Optical Thickness (Ta) as is defined from the following formula, was used:

$$\mathrm{AAOT}(\lambda) = \mathrm{AOT}(\lambda) * [1 - \mathrm{SSA}_{(340\,\mathrm{nm})}] \quad (4)$$

The methodologies shown below are based on the dependence of RT to AAOT and can be: (a) experimental, using the results of GB and OMI measurements and (b) theoretical, using radiative transfer model calculations.

The experimental method is based on the investigation of a similar TOMS to GB bias presented in Arola et al. (2005) which here is performed by comparing GB and OMI data under clear sky conditions. In Fig. 3 the ratio OMI versus GB measurements at 324 nm under clear sky conditions is shown against AAOT.

The AOT is measured within ±30 min from the OMI overpass at 324 nm and the SSA is derived from Brewer irradiance measurements based on the methodology by Bais et al. (2005). The calculated slope was found equal with 2.1 per unit of AAOT and with an intercept of 1.07. Using this slope we investigated if such a correction could improve the observed bias showed in Table 1. In addition, results presented by Krotkov et al. (2005), that calculated RT through AOT, and SSA measurements at Washington area for TOMS satellite, proposed a similar correction using the formula:

$$C_A = [1 + 3 * \mathrm{AAOT}(\lambda)]^{-1} \quad (5)$$

The method presented above is solar zenith angle independent. However, the effects of an aerosol absorbing layer will lead to higher UV attenuation at higher solar zenith

ACPD
8, 17467–17493, 2008

angles due to the increased optical path of the solar photons through this layer. For that purpose we tried to eliminate the solar zenith angle effect on aerosol absorption following an idea of Garcia et al. (2006). We used slant absorption optical thickness (AAOTS) instead of AAOT, which is defined as:

$$\text{AAOTS} = \text{AAOT}/\cos(\text{sza}) \quad (6)$$

where sza is the solar zenith angle. Using the same dataset presented in Fig. 3 we calculated the RT dependence on AAOTS, shown in Fig. 4.

This method provides a new slope of 1.6 per unit of aerosol slant column absorption optical thickness and an intercept of 1.06. The solar zenith angle impact on the effect of aerosol in the UV irradiance is crucial especially for locations with annual AOT and SSA variations. As an example, the case of Thessaloniki where AOT measurements show a summer AOD maximum with mean values almost double than those observed during the winter months (Kazadzis et al., 2007). However, measurements over the city show enhanced SSA in wintertime leading to the increase of AAOT according to formula 1 which results in an almost constant AAOT during the year (Arola et al., 2005). In addition, as the OMI overpass time is almost constant throughout the year, wintertime measurements are performed at higher solar zenith angles than the ones in summertime. All the above are not taken into consideration in the first method and could lead to comparable UV attenuation due to aerosols in winter and in summer despite the fact that AOT is higher in summertime.

Another approach that was investigated was to calculate C_A with the use of model calculations. The absorbing aerosol layers that are "invisible" for the OMI instrument lead to the underestimation of the attenuation of UV irradiance reaching the ground. With the help of the Libradtran radiative transfer model we constructed look up tables (LUT) quantifying aerosol scattering and absorption due to an aerosol layer. An example is shown in Figs. 5a and 5b: Lines in Fig. 5a represent the UV irradiance ratio $E_{clear(CT=1)}/E_{aero}$, where E_{aero} is the UV irradiance calculated with the help of the LUT's for various SSA,and AOT cases. This ratio is presented here as a function of AOT

ACPD
8, 17467–17493, 2008

and SSA for a constant solar zenith angle of 40° and total column ozone of 340 DU. As expected the higher the AOT and the lower the SSA, lead to higher correction factors calculated. For a certain case of SSA (0.88 at 340 nm) and AOT of 0.5 at 340 nm the correction factor shown in Fig. 5b is ~17%. While ~6.5% of this is due to aerosol scattering (that is already taken into account on the OMI correction through C_T) and ~10.5% due to aerosol absorption, for UV irradiance at 324 nm.

All the above methods include the premise that various parameters like AOT and SSA in the UV (preferably) or in the visible (through AERONET data) have to be known in order to be used for calculating C_A on a global scale. We have used Thessaloniki data to investigate how the C_A statistics derived from the theoretical method are altered when using a constant (climatological) AOT and SSA. For this purpose we have used synchronous AOT Brewer measurements at 340 nm and a mean SSA (0.91) at 440 nm for the 2004–2007 period (Kazadzis et al., 2007), derived from a CIMEL sunphotometer. Through the calculated LUT's we have retrieved C_A using cloud-free days only. The results of the statistics for all of the above correction methods are provided in the following Table 2:

The results presented in Table 2 are the OMI–GB ratios after applying each method's calculated C_A's. All methods presented here lead to an improvement of the OMI–GB bias. Especially method #3 (shown in this table), that is described by formula (5), provides the best correction approach. The use of either of the aforementioned methods by any ground-based measuring station depends on the availability of independent aerosol optical properties data (AOT, SSA).

We have tried to investigate possible dependence of solar zenith angle, aerosol optical thickness, absorption optical thickness, ozone or time to the original and correction applied datasets. No systematic dependence of C_A to the above parameters was found. As an example, the results of the application of the above methods to the time series of RT measurements are shown in the following Fig. 6.

Using the C_A's retrieved by method #3 (on Table 2) we have calculated corrected OMI UV irradiances for 305 nm, 324 nm and 380 nm which are presented in Fig. 7:

ACPD
8, 17467–17493, 2008

Confirming further the results of Table 2, the coefficients of determination calculated after applying the corrections are much improved. It has to be mentioned that the number of the original cases shown in Fig. 7 is 267 (cloudless cases over 3.5 years period), while the corrected ones are only 201 due to the absence of coincident aerosol optical thickness measurements within one hour from the OMI overpass.

5 Discussion and conclusions

Three and a half years of the operational OMI UV data and Brewer UV irradiance measurements were compared for the area of Thessaloniki, Greece. Largest positive OMI biases were found at 305 nm that reach 32% and 27% for cloudy and cloudless measurements. Smaller biases were found for UVA wavelengths: 20% and 16% at 324 nm and 16% and 11% at 380 nm, respectively. The biases were attributed to the absorption of aerosols not taken into account from the OMI algorithm.

Various methods have been tested in order to investigate the possibility of an OMI UV data post correction for absorbing aerosols. All methods presented here lead to improved OMI-GB comparisons. Using AOT measurements at the exact wavelengths analyzed and SSA measurements at 340 nm the correction methodologies were compared. Results showed that for 305 nm the averaged correction C_A is compensating for most of the observed overestimation while for 324 nm and for 380 nm the correction methods eliminate most of the observed biases.

The post correction factors, C_A calculated for Thessaloniki area using formula 5 are in the order of 0.8, 0.88 and 0.9 for 305 nm, 324 nm and 380 nm, respectively. Such values can be used for urban areas with similar or measured aerosol optical properties. Using the slopes of RT as a function of AAOT, measured at Thessaloniki, there remains a 9%, 6% and 4% positive OMI bias not related to aerosol absorption. A possible explanation for this could be the fact that in cloudless cases, absorbing aerosols attenuate also the reflected irradiance from the ground. That could lead to a small underestimation of LER resulting to a small C_T overestimation (see Eq. 2). The final estimated

ACPD
8, 17467–17493, 2008

surface irradiance from OMI will be overestimated especially at low SSA cases. On the contrary, using formula (5) which introduces a larger slope than the one measured, in a way, this effect is eliminated. Spectral differences of methods 1 and 2 presented in Table 2 can be also a result of spectral dependence of the SSA.

Comparing total column ozone values retrieved from OMI and GB measurements we found a small OMI ozone under-estimation in the order of 1.2% (mean), which can be also have a (smal) effect to all OMI–GB comparisons, especially at 305 nm.

Model calculations using measurements of a CIMEL sun-photometer were introduced because of the availability of such measurements (especially SSA) from the specific instruments worldwide. The method retrieves larger C_A and the corrected RT's still show OMI overestimation especially for lower wavelengths. One possible explanation for the above results could be the spectral dependence of SSA. Previous works (Krotkov et al., 2005) indicated that SSA could be less in UVB than in the visible wavelength range especially at the urban area under investigation. This SSA effect becomes more complicated when considering seasonal variations of absorbing aerosol properties. As the mean SSA at 440 nm for the area is 0.91 using a value of 0.88 for correction at 380 nm, leads to a few per cent differences among the corrected OMI irradiances and the GB ones. However, an SSA value that could be used for achieving similar results for the 305nm irradiance would be approximately 0.84. Measurements of SSA in the UVB are still uncertain especially when AOT is low and further investigation on the absorbing aerosol and gaseous (NO_2, SO_2) properties at these wavelengths is still an intriguing scientific future issue.

The standard deviation for all cloudless OMI vs Brewer ratios were found to be reasonable, taking into account possible OMI sub-pixel variability of AOT and thus UV irradiances. Results of OMI sub-pixel UV variability showed that for pixels that include urban areas UV variability can be as high as 20% even for cloudless conditions. While a similar campaign in a non urban environment (Weihs et al., 2008) showed that for cloudy conditions UV variability can reach 50%. The above results show the limitations when comparing satellite with single point GB measurements.

For the case of cloudy conditions the OMI–Brewer ratios showed approximately 5% higher values than the cloud-free ones and in addition higher standard deviation. For the higher values the explanation is the high UV irradiance variability under cloudy conditions and the absence of information on the amount of the direct sun attenuation for each individual measurement. An additional reason is the fact that OMI overpasses and GB spectral measurements are not exactly synchronous, which is important issue comparing UV measurements under a variable radiation field. The absolute level differences and their spectral dependence indicate that similar C_A's have to be applied in cloudy cases too. However, the UV attenuation due to aerosol absorption under cloudy conditions is more difficult to be studied theoretically, as more information about the clouds and the aerosol layer height are necessary. In addition, aerosol absorption is difficult to be quantified as sun-photometric measurements fail under cloudy conditions. In this case, the calculated C_A's can be used, or other possible correction procedures have to be considered.

Post processing algorithms for OMI-UV products have to be employed when using OMI data for regions with high aerosol load. Simple parameters for public use (e.g. UV Index) can be overestimated by more than 20% if using OMI overpass data for urban areas such as Thessaloniki. The use of climatological mean values of AOT and absorption (SSA) aerosol quantities in a global scale could be used based in one of the methodologies presented in this work. Finally, when it is possible, the spectral dependence of AOT and SSA has to be taken into account in order to include a correction for the spectral dependence of UV attenuation reaching the ground, in the presence of an aerosol layer.

Acknowledgements. The Dutch-Finnish built OMI instrument is part of the NASA EOS Aura satellite payload. The OMI project is managed by NIVR and KNMI in the Netherlands. We thank the OMI International Science Team for the satellite data used in this study.

Stelios Kazadzis would like to acknowledge the Marie Curie Intra European fellowship "Validation of Aerosol optical Properties and surface Irradiance measured from Ozone Monitoring Instrument on board of AURA satellite" VAP-OMI, AOR A/119693 - PIEF-GA-2008-219908.

References

Arola, A., Kazadzis, S., Krotkov, N., Bais, A., Gröbner, J., and Herman, J. R.: Assessment of TOMS UV bias due to absorbing aerosols, J. Geophys. Res.-Atmos., 110 (23), 1–7, 2005.

Amiridis, V., Balis, D. S., Kazadzis, S., Bais, A., Giannakaki, E., Papayannis, A., and Zerefos, C.: Four-year aerosol observations with a Raman lidar at Thessaloniki, Greece, in the framework of European aerosol Research Lidar Network (EARLINET), J. Geophys. Res., 110 (D21), D21203, doi:10.1029/2005JD006190, 2005.

Bais, A. F., Kazantzidis, A., Kazadzis, S., Balis, D. S., Zerefos, C. S., and Meleti, C.: Deriving an effective aerosol single scattering albedo from spectral surface UV irradiance measurements, Atmos. Environ., 39 (6), 1093–1102, 2005.

Bhartia, P. K., J. Herman, R. D. McPeters, and Torres, O.: Effect of Mount Pinatubo aerosols on total ozone measurements from backscatter ultraviolet (BUV) experiments, J. Geophys. Res., 98 (D10), 18 547–18 554, 1993.

Bhartia, P. K. and Wellemeyer, C. W.: TOMS-V8 total O3 algorithm, in OMI Algorithm Theoretical Basis Document, NASA Goddard Space Flight Cent., Greenbelt, Md., 1–91, 2002.

Chubarova N.: Influence of Aerosol and Atmospheric Gases on Ultraviolet Radiation in Different Optical Conditions Including Smoky Mist of 2002, Doklady Earth Sciences, 394, 1, 2004, 62–67, Translated from Doklady Akademii Nauk, 394, 1, 105–111, 2004.

Eck, T. F., Holben, B. N., Dubovik, O., Smirnov, A., Goloub, P., Chen, H. B., Chatenet, B., Gomes, L., Zhang, X. Y., Tsay, S. C., Ji, Q., Giles, D., and Slutsker, I.: Columnar aerosol optical properties at AERONET sites in central eastern Asia and aerosol transport to the tropical mid-Pacific, J. Geophys. Res.-Atmos., 110 (6), 1–18, 2005.

Fioletov, V. E., Kerr, J. B., Wardle, D. I., Krotkov, N., and Herman, J. R.: Comparison of Brewer ultraviolet irradiance measurements with total ozone mapping spectrometer satellite retrievals, Opt. Eng., 41 (12), 3051–3061, 2002.

Garane, K., Bais, A. F., Kazadzis, S., Kazantzidis, A., and Meleti, C.: Monitoring of UV spectral irradiance at Thessaloniki (1990–2005): Data re-evaluation and quality control, Ann. Geophys., 24 (12), 3215–3228, 2006.

García, O. E., Díaz, A. M., Expósito, F. J., Díaz, J. P., Gröbner, J., and Fioletov, V. E.: Cloudless aerosol forcing efficiency in the UV region from AERONET and WOUDC databases, Geophys. Res. Lett., 33, L23803, doi:10.1029/2006GL026794, 2006.

Herman, J. R., Krotkov, N., Celarier, E., Larko, D., and Labow, G.: Distribution of UV radiation

at the Earth's surface from TOMS-measured UV-backscattered radiances, J. Geophys. Res.-Atmos., 104 (D10), 12 059–12 076, 1999.
Ialongo, I., Casale, G. R., and Siani, A. M.: Comparison of total ozone and erythemal UV data from OMI with ground-based measurements at Rome station, Atmos. Chem. Phys., 8, 3283–3289, 2008, http://www.atmos-chem-phys.net/8/3283/2008/.
Kazadzis, S., Bais, A., Amiridis, V., Balis, D., Meleti, C., Kouremeti, N., Zerefos, C. S., Rapsomanikis, S., Petrakakis, M., Kelesis, A., Tzoumaka, P., and Kelektsoglou, K.: Nine years of UV aerosol optical depth measurements at Thessaloniki, Greece, Atmos. Chem. Phys., 7, 2091–2101, 2007, http://www.atmos-chem-phys.net/7/2091/2007/.
Kazantzidis, A., Bais, A. F., Gröbner, J., Herman, J. R., Kazadzis, S., Krotkov, N., Kyro, E., den Outer, P. N., Garane, K., Görts, P., Lakkala, K., Meleti, C., Slaper, H., Tax, R. B., Turunen, T., and Zerefos, C. S.: Comparison of satellite-derived UV irradiances with ground-based measurements at four European stations, J. Geophys. Res.-Atmos., 111 (13), D13207, doi:10.1029/2005JD006672, 2006.
Koukouli, M. E., Balis, D. S., Amiridis, V., Kazadzis, S., Bais, A., Nickovic, S., and Torres, O.: Aerosol variability over Thessaloniki using ground based remote sensing observations and the TOMS aerosol index, Atmos. Environ., 40, 5367–5378, 2006.
Krotkov, N. A., Bhartia, P. K., Herman, J. R., Fioletov, V., and Kerr, J.: Satellite estimation of spectral surface UV irradiance in the presence of tropospheric aerosols 1. Cloud-free case, J. Geophys. Res.-Atmos., 103 (D8), 8779–8793, 1998.
Krotkov, N. A., Herman, J. R., Bhartia, P. K., Fioletov, V., and Ahmad, Z.: Satellite estimation of spectral surface UV irradiance 2. Effects of homogeneous clouds and snow, J. Geophys. Res.-Atmos., 106 (D11), 11 743–11 759, 2001.
Krotkov, N., Herman, J., Bhartia, P. K., Seftor, C., Arola, A., Kaurola, J., , Kalliskota, S., Taalas, P., and Geogdzhaev, I. V.: Version 2 total ozone mapping spectrometer ultraviolet algorithm: Problems and enhancements, Opt. Eng., 41 (12), 3028–3039, 2002.
Krotkov, N., Bhartia, P. K., Herman, J., Slusser, J., Scott, G., Labow, G., Vasilkov, A. P., Eck, T. F., Dubovik, O., and Holben, B. N.: Aerosol ultraviolet absorption experiment (2002 to 2004), part 2: Absorption optical thickness, refractive index, and single scattering albedo, Opt. Eng., 44 (4), 1–17, 2005.
Levelt, P. F., Hilsenrath, E., Leppelmeier, G. W., Van Den Oord, G. H. J., Bhartia, P. K., Tamminen, J., De Haan, J. F., and Veefkind, J. P.: Science objectives of the ozone monitoring instrument, IEEE T. Geosci. Remote, 44 (5), 1199–1207, 2006.

Marenco, F., Santacesaria, V., Bais, A. F., Balis, D., Di Sarra, A., Papayannis, A., and Zerefos, C.: Optical properties of tropospheric aerosols determined by lidar and spectrophotometric measurements (Photochemical Activity and Solar Ultraviolet Radiation Campaign), Appl. Optics, 36 (27), 6875–6886, 1997.

Mayer, B. and Kylling, A.: Technical note: The libRadtran software package for radiative transfer calculations – Description and examples of use, Atmos. Chem. Phys., 5, 1855–1877, 2005, http://www.atmos-chem-phys.net/5/1855/2005/.

McKenzie, R. L., Seckmeyer, G., Bais, A. F., Kerr, J. B., and Madronich, S.: Satellite retrievals of erythemal UV dose compared with ground-based measurements at northern and southern midlatitudes, J. Geophys. Res.-Atmos., 106 (D20), 24 051–24 062, 2001.

Slaper, H., Reinen, H. A. J. M., Blumthaler, M., Huber, M., and Kuik, F.: Comparing ground-level spectrally resolved solar UV measurements using various instruments: a technique resolving effects of wavelength shift and slit width, Geophys. Res. Lett., 22 (20), 2721–2724, 1995.

Tanskanen, A., Krotkov, N. A., Herman, J. R., and Arola, A.: Surface ultraviolet irradiance from OMI, IEEE T. Geosci. Remote, 44 (5), 1267–1271, 2006.

Tanskanen, A., Lindfors, A., Määttä, A., Krotkov, N., Herman, J., Kaurola, J., Koskela, T., Lakkala, K., Fioletov, V., Bernhard, G., McKenzie, R., Kondo, Y., O'Neill, M., Slaper, H., DenOuter, P., Bais, A. F., and Tamminen, J.: Validation of daily erythemal doses from ozone Monitoring Instrument with ground-based UV measurement data, J. Geophys. Res., 5, 112, D24S44, doi:10.1029/2007JD008830, 2008.

Vasaras, A., Bais, A. F., Feister, U., and Zerefos, C. S.: Comparison of two methods for cloud flagging of spectral UV measurements, Atmos. Res., 57 (1), 31–42, 2001.

Weihs, P., Blumthaler, M., Rieder, H. E., Kreuter, A., Simic, S., Laube, W., Schmalwieser, A. W., Wagner, J., and Tanskanen, A.: Measurements of UV irradiance within the area of one satellite pixel, Atmos. Chem. Phys., 8, 5615–5626, 2008, http://www.atmos-chem-phys.net/8/5615/2008/.

Wuttke, S., Verdebout, J., and Seckmeyer, G.: An Improved Algorithm for Satellite-derived UV Radiation, Photochem. Photobiol., 77 (1), 52–57, 2003.

World Meteorological Organization (WMO): Scientific Assessment of Ozone Depletion: 2006, Global Ozone Research and Monitoring Project, WMO Rep. N, 47, Geneva, 2007.

Table 1. RT statistics.

Wavelength (nm)	*All data*				*Cloudy*				*Cloudless*				E_{clear}/ *GB Brewer*			
	m	R^2	W_{10}	W_{20}	*M*	R^2	W_{10}	W_{20}	*m*	R^2	W_{10}	W_{20}	*m*	R^2	W_{10}	W_{20}
305	*1.30*	0.94	43.3	68.2	*1.32*	0.91	32.4	57.7	*1.27*	0.95	64.8	87.6	*1.31*	0.95	64.1	89.4
324	*1.17*	0.89	51.3	73.1	*1.20*	0.85	38.8	62.5	*1.15*	0.90	76.9	92.4	*1.17*	0.90	80.1	93.5
380	*1.13*	0.89	47.2	70.7	*1.16*	0.85	37.4	61.6	*1.11*	0.90	71.8	89.7	*1.14*	0.89	72.5	91.5
CIED	*1.20*	0.93	51.5	75.4	*1.22*	0.89	40.5	68.1	*1.19*	0.95	75.0	91.9	*1.21*	0.95	74.7	93.7

m: median, R^2: coefficient of determination, *Wi*: per cent of cases ranging within ±i% from the median.

Table 2. Results of the methodologies investigated.

#	Method	305 nm RT (1σ)	324 nm RT (1σ)	380 nm RT (1σ)
	No correction	1.27 (0.15)	1.15 (0.10)	1.11 (0.12)
1	$[1 + 2.1 * AAOT(\lambda)]^{-1}$	1.09 (0.11)	1.06 (0.07)	1.04 (0.09)
2	$[1 + 1.6 * AAOTS(\lambda)]^{-1}$	1.08 (0.11)	1.05 (0.10)	1.03 (0.13)
3	$[1 + 3 * AAOT(\lambda)]^{-1}$	1.04 (0.11)	1.02 (0.07)	1.00 (0.10)
4	Constant SSA at 440nm	1.14 (0.13)	1.06 (0.09)	1.03 (0.10)

ACPD
8, 17467–17493, 2008

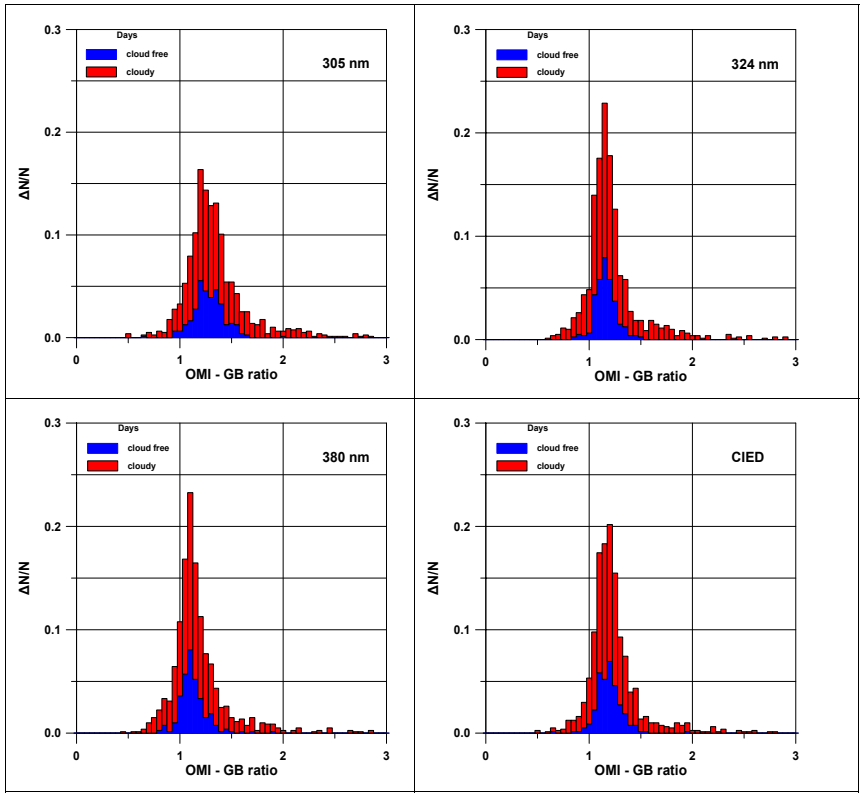

Fig. 1. Distributions-histograms of the ratio of the satellite-derived to those determined from the ground-based UV measurements (305 nm up-left, 324 nm up-right, 380 nm down-left and erythemally weighted dose down-right). Blue bars correspond to days with cloud-free conditions, while measurements under cloudy conditions are plotted in red.

ACPD
8, 17467–17493, 2008

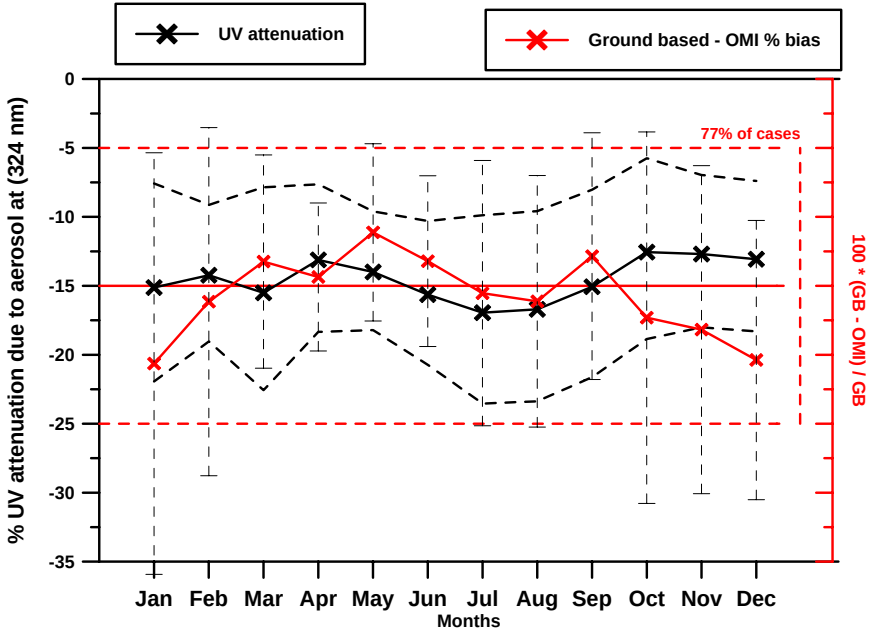

Fig. 2. Calculated UV attenuation due to aerosols (Black line) and OMI-GB UV bias at 324 nm at Thessaloniki Greece (red line). Dash lines represent the 1σ AOT variability due to the use of the monthly mean aerosol optical thickness values. Black error bars represent the 1σ of the calculated monthly mean UV attenuation. Red line represents the mean % GB – OMI difference and red dashed lines the range that 77% of all OMI-GB compared cases lie within.

ACPD
8, 17467–17493, 2008

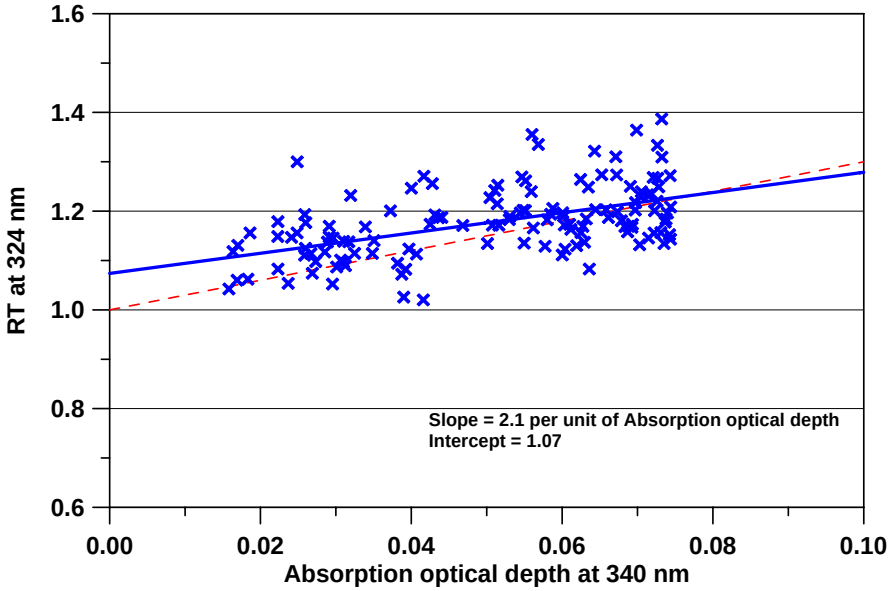

Fig. 3. OMI–GB ratio at 324 nm for cloudless cases as a function of AAOT. The blue line is a linear regression on the data. The correction of Krotkov et al. (2005) is also shown (red line).

ACPD
8, 17467–17493, 2008

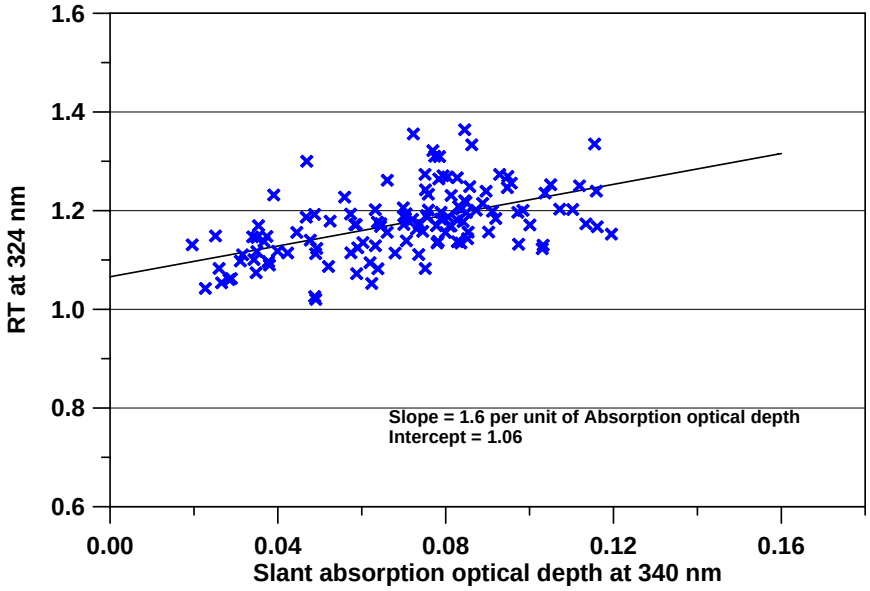

Fig. 4. OMI–GB ratio at 324 nm for cloudless cases as a function of AAOTS. The black line is a linear regression on the data.

ACPD
8, 17467–17493, 2008

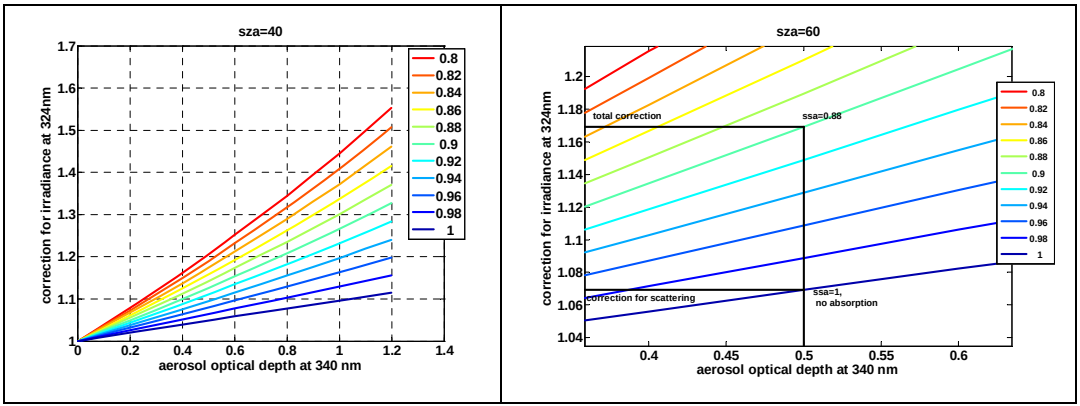

Fig. 5. Radiative model calculations of UV attenuation $E_{clear(CT=1)}$ / E_{aero}, for various AOT and SSA values (left). The ratios $E_{clear(CT=1)}$ / E_{aero}, for a constant solar zenith angle (60°) and (SSA,AOT)=(0.88, 0.5) at 340 nm.

ACPD
8, 17467–17493, 2008

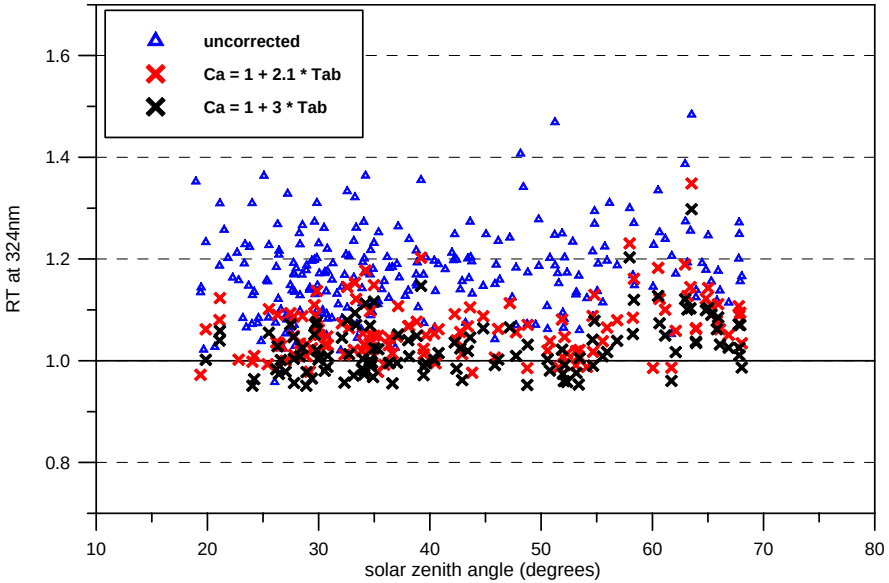

Fig. 6. OMI–GB ratio at 324 nm as a function of solar zenith angle. Blue symbols represent the original data and red and black the results of corrections 1 and 3 shown in Table 2.

ACPD
8, 17467–17493, 2008

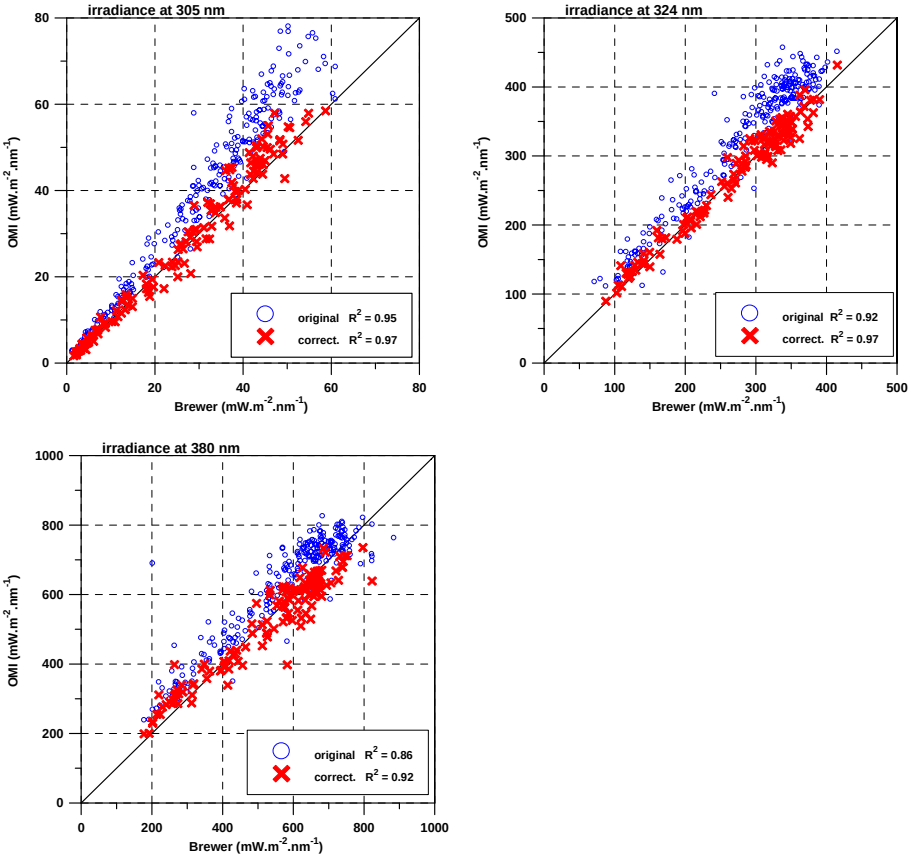

Fig. 7. OMI and Brewer spectral irradiance measurements for 305 nm (upper left), 324 nm (upper right) and 380 nm (down) under cloudless skies. Blue symbols represent the original data and red the OMI corrected ones.

ACPD
8, 17467–17493, 2008